Active faults in the Sea of Marmara, western Turkey, imaged by seismic reflection profiles

J. R. Parke[1]*, T. A. Minshull[1], G. Anderson[1], R. S. White[1], D. McKenzie[1], I. Kuşçu[2], J. M. Bull[3], N. Görür[4] and C. Şengör[4]

[1]*Bullard Laboratories, Madingley Road, Cambridge CB3 0EZ, UK,* [2]*Maden Tetkik ve Arama Genel Müdürlügü, Ankara, Turkey,* [3]*Southampton Oceanography Centre, Southampton SO14 32H, UK,* [4] *ITÜ Maden Fakültesi, Jeoloji Bölümü, Ayazaga 80626, Istanbul, Turkey*

ABSTRACT

Turkey is moving westward relative to Eurasia, thereby accommodating the collision between Arabia and Eurasia. This motion is mostly taken up by strike-slip deformation along the North and East Anatolian Faults. The Sea of Marmara lies over the direct westward continuation of the North Anatolian Fault zone. Just east of the Sea of Marmara, the North Anatolian Fault splits into three strands, two of which continue into the sea. While the locations of the faults are well constrained on land, it has not yet been determined how the deformation is transferred across the Sea of Marmara, onto the faults on the west coast of Turkey. We present results from a seismic reflection survey undertaken to map the faults as they continue through the three deep Marmara Sea basins of Çınarcık, Central Marmara and Tekirdağ, in order to determine how the deformation is distributed across the Sea of Marmara, and how it is taken up on the western side of the sea. The data show active dipping faults with associated tilting of sedimentary layers, connecting the North Anatolian Fault to strike-slip faults that cut the Biğa and Gallipoli Peninsulas.

Terra Nova, 11, 223–227, 1999

Introduction

The Eastern Mediterranean is one of the world's most seismically active regions. Global kinematic models (NUVEL-1 A, Demets *et al*., 1990) based on the analysis of oceanic spreading, fault systems, and earthquake slip vectors, indicate that Arabia is moving in a NNW direction relative to Eurasia at an average rate of about 25 mm yr^{-1}. GPS data show an upper limit to the right-lateral movement across the North Anatolian Fault Zone of 30 mm yr^{-1}, and this value is higher than that estimated from long-term geological features (Reilinger *et al*., 1997). As a result of the collision between Arabia and Eurasia, Turkey is being thrust westward over the African oceanic plate along the Hellenic Arc. The motion of Turkey relative to Eurasia and Arabia is taken up principally by strike-slip deformation along the North and East Anatolian Faults [Fig. 1(a), inset].

In this paper we examine the connection between the westward motion of Turkey relative to Eurasia, and the distributed deformation and extension observed in the Sea of Marmara. Across most of Turkey, the motion between Turkey and Eurasia is taken up on the North Anatolian Fault, a relatively simple, narrow, right-lateral strike-slip fault zone; the high plateau of central Turkey to the south may be considered as a relatively rigid block (Reilinger *et al*., 1997). This fault zone is thought to have first become active in the late Miocene to Pliocene (Şengör *et al*., 1985). The total amount of displacement is still uncertain, ranging from estimates of 35–40 km (Barka and Kadinsky-Cade, 1988) to above 80 km (Şengör, 1979).

Just east of the Sea of Marmara, the North Anatolian Fault splits into three strands; a southern strand between Yenisehir and Manyas; a middle strand (Gemlik fault) that skirts the southeastern Marmara shoreline from Iznik to Bandırma, and the northern strand (Çınarcık fault) which bounds the southern edge of the Gulf of Izmit and traverses the deep Marmara basin to bound the southern edge of the Gulf of Saros to the west [Fig. 1]. The three strands have geometrically similar patterns but historical records (Ambraseys, 1988) indicate that the northernmost strand has shown more seismic activity in the last 20 centuries.

Previous attempts to produce maps of the fault distribution in the Sea of Marmara include work by Barka and Kadinsky-Cade (1988), Smith *et al*. (1995) and Wong *et al*. (1995). Smith *et al*. (1995) attribute the greater width of the southern shelf compared to the north to a much greater sediment flux from the south, and conclude that this exaggerates the apparent tectonic activity of the deep northern basins. Wong *et al*. (1995) partition the deep Marmara basin into five tectonic blocks, describing three of them as pull-apart basins, and the remaining two as transpressional push-up structures, which separate the basins.

In order to determine more accurately the locations of faults, and how they interact, we conducted a four week seismic reflection profiling survey in September 1997. We recorded over 2000 km of high-resolution 2D reflection data, using a 10-gun, 23 L, tuned generator-injector compressed air source. The hydrophone had 96 channels, extending to a maximum offset of 1500 m from the ship. In order to reduce noise from the ships' engines, the data were bandpass filtered at 8–218Hz at the acquisition stage. Shots were fired at a spacing of 50 m. The data were recorded to a two-way time (TWT) of 8 s, at a sample interval of 2 ms. Navigation was by Differential Global Positioning System (DGPS), with an onshore VHF radio beacon, allowing a location accuracy of $\pm$ 5 m.

Good images of the top 2–3 km of the subsurface were acquired, with occasional deeper reflectors also observed. The data were of excellent quality in the deep water regions, permitting clear images of faults cutting recent seafloor sediments, as well as some less active faults, now buried beneath several kilometres of sediment. In the shallower, southern shelf regions, quality deteriorated due to interference from strong water multiples. These strong multiples suggest a large impedance contrast

Correspondence: Tel: +44/1223-337180; Fax: +44/1223-360779;
E-mail: parke@esc.cam.ac.uk

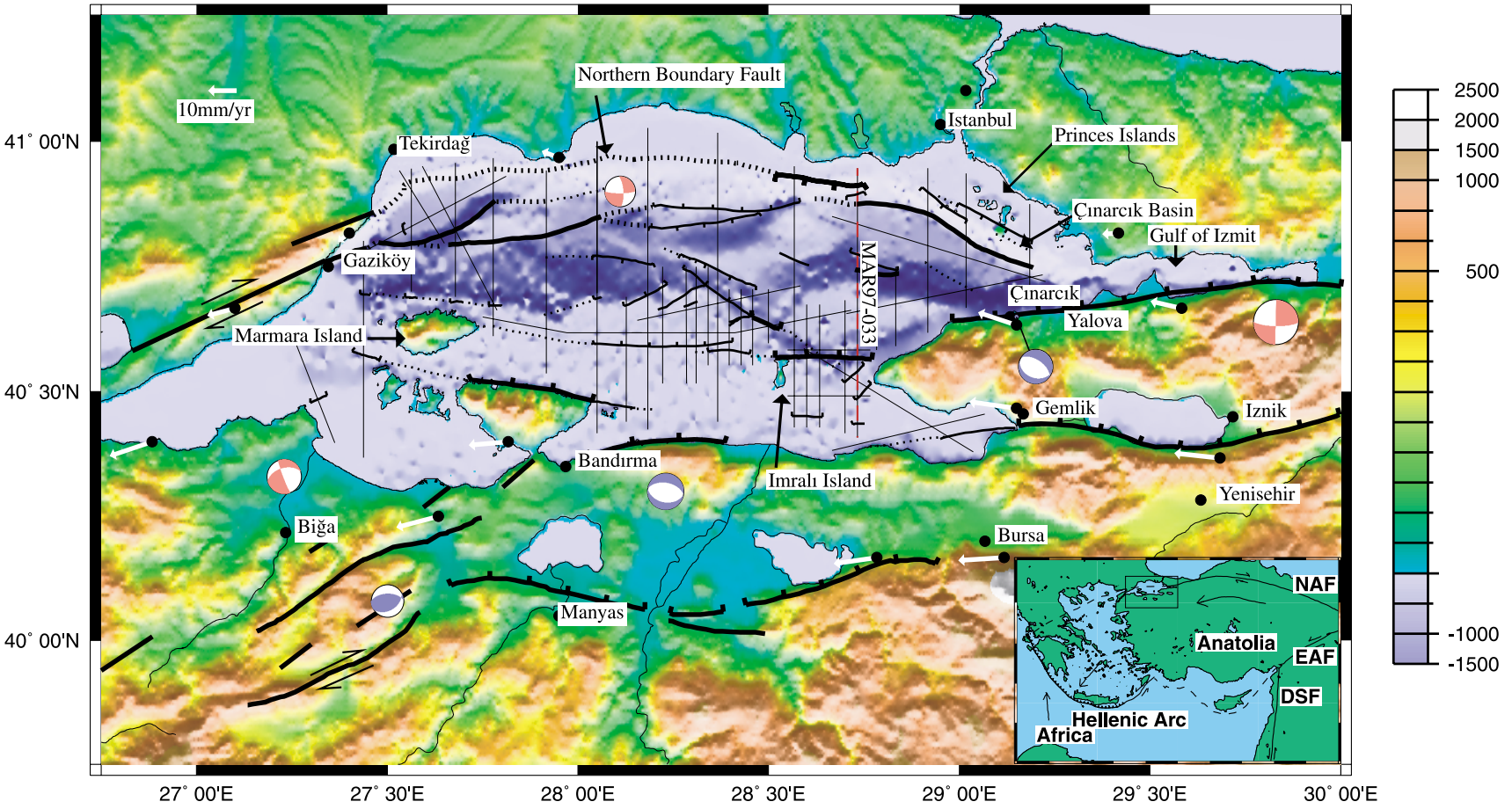

Fig. 1 Topographic map of the Sea of Marmara with locations of observed faults on land (Saroglu *et al.*, 1992) and the main offshore faults from interpreted seismic reflection profiles. Topographic data are from the GTOPO30 global database, and bathymetric data from Turkish Admiralty sources. Large faults cutting recent sediments are shown in solid black lines. Tracklines from the survey reported here are shown as thin solid lines. Line MAR97-033 (Fig. 2.) is shown as a thin dashed red line. The inset provides an overview of the plate motions in the Eastern Mediterranean. Shown are the North Anatolian Fault (NAF), East Anatolian Fault (EAF), Dead Sea Fault (DSF), and the Hellenic Arc. CMT solutions are plotted in red, P and SH wave modelling solutions in blue, taken from Taymaz *et al.* (1991). GPS velocities are shown in white (Straub *et al.* (1997).

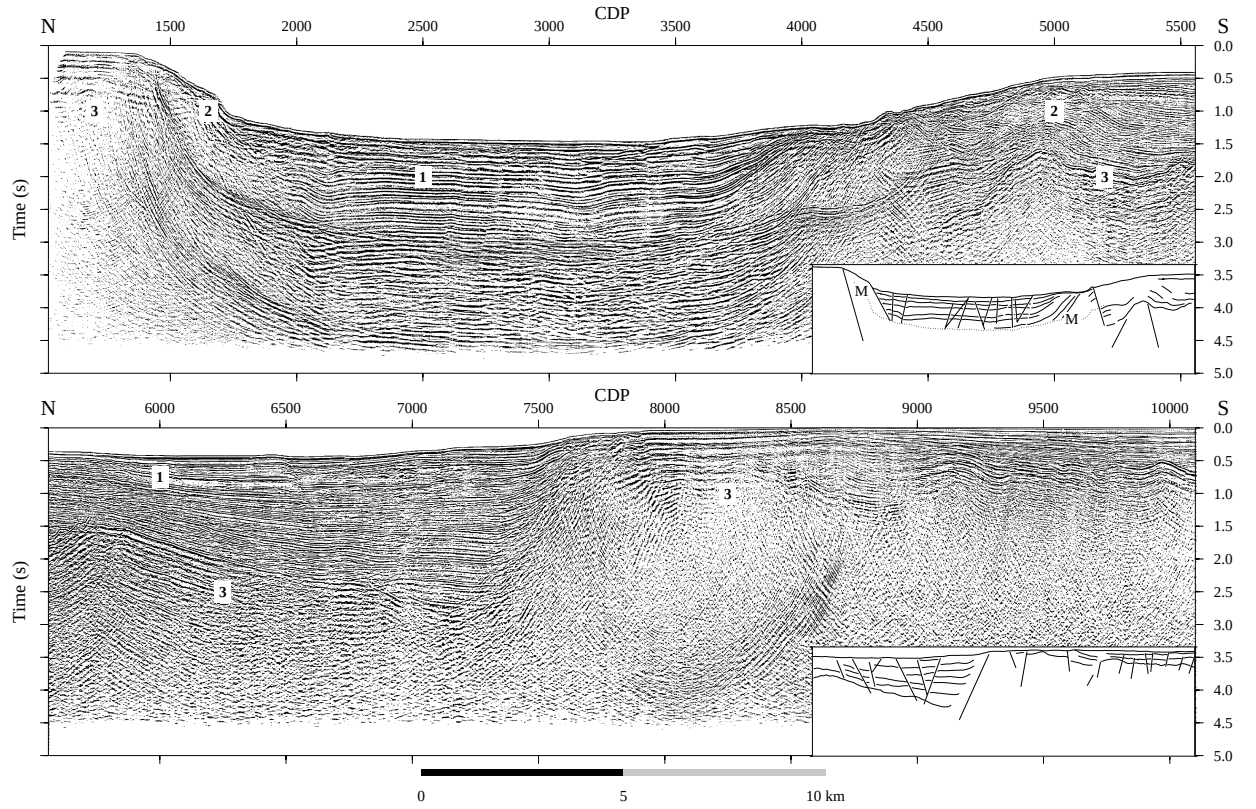

Fig. 2 A representative seismic reflection profile; Line MAR97-033. Vertical exaggeration at the seabed is 2: 1. Inset in each section is an interpretation, showing major faults and sedimentary horizons. 'M' is the seabed multiple. Units 1–3 as discussed in the main text are marked on the sections.

between the water and the seafloor, indicating that the southern shelf may be made of older, more consolidated sediment. Some residual bubble pulse energy is also evident in the data.

This paper concentrates on mapping the faults in the deeper regions, and how they connect across the Sea; we illustrate the quality of our data by presenting profile MAR97–033 [Fig. 2] which runs across the eastern Sea of Marmara.

Data reduction

Prior to stacking the data, the far offset channels were muted to remove refracted arrivals from shallow sediments. For normal moveout correction, a simple initial basic velocity model was calculated, with a uniform velocity of 1500 m s^{-1} down to the sea-floor. An interval of 500 ms after the seafloor reflection, the interval velocity was set at 1800 m s^{-1}, with further fixed values of 2500 m s^{-1} and 4000 m s^{-1} at 1000 ms intervals, to give isovelocity contours parallel to the seabed. This model worked well in the large, flat-lying sedimentary expanses of the deep basins, although in some areas deeper basement features could be observed, and here more accurate picking of velocities based on semblance analysis was justified. In these areas, the velocity contours beneath the deepest pick were set to follow a deeper basement reflector, independent of the seafloor. A steeper velocity gradient was used on the shallow southern shelf, where relatively few accurate velocity determinations could be obtained because of the poor quality of the deeper reflections. The data were then stacked, and additional filters applied to remove noise. Finally the data were Stolt migrated, at 1500 m s^{-1} (Stolt, 1978).

The multichannel data were analysed in migrated and unmigrated time sections, to 5 s TWT. They were used primarily to identify units and structures at depth, and hence to trace the faults through the Sea of Marmara.

Fault map

A total of 40 reflection profiles was recorded across the Sea of Marmara (Fig. 1). A general survey of the area, with long N–S lines 10 km apart was undertaken, with smaller, local lines, spaced 2–3 km apart, in locations where active faults might be expected to cut surface sediments, or where sediment cover was sufficiently thick to give a record of events in the area. Several different stratigraphic units could be identified and traced from line to line.

These included:

1 *Unit 1* (Fig. 2). Relatively recent flat-lying or draped sediments, which have filled in the deeper basins, but have limited and patchy cover in the shallower water areas.

2 *Unit 2* (Fig. 2). Convoluted sediments. These have been buried by the more recent sediments in places, although in others they are exposed and display erosional surfaces. Folding or lateral compression is also observed.

3 Underlying units (1) and (2) is an attenuative basement unit (*Unit 3*). The top of this appears as a continuous, high-amplitude reflector, accompanied by diffraction hyperbolae. It appears as a deep reflector in the southern shelf but is exposed in places at the edges of the deeper basins in the north.

In this paper we use these units as an aid to mapping the locations of the fault zones connecting the Çınarcık fault to the Saros-Gaziköy fault. The three units are all present in line MAR97-033 (Fig. 2).

Based on historical seismicity, the northernmost strand of the North Anatolian Fault, the Çınarcık fault, appears to be more active than the Gemlik fault to the south (Ambraseys, 1988). Directly north of Çınarcık, a zone of distributed deformation, where sediments are disturbed in a region about 1 km wide is observed on the northern edge of the Çinarcik basin. This zone resolves itself into two strands which continue westward, forming the bounding faults on the easternmost basin. It is this basin which is crossed by line MAR97-033. The northernmost of the two strands splits again, and the resulting faults continue across the Sea of Marmara, bounding the westernmost basin, and connecting directly with the Saros-Gaziköy fault system. Distributed deformation can be observed in areas where a fault splits into two strands. *En echelon* faults are also seen, stepping around the edges of the basins. Faults also terminate as the motion is taken up by neighbouring faults to the north or south.

Seismic profile

Line MAR97-033 (Fig. 2) is a long regional line, in a N–S direction, at the eastern end of the Sea of Marmara. It was shot in order to provide a constraint on the locations of the two major strands of the North Anatolian Fault as they enter the sea. It also exhibits features which recur on other profiles and are useful for mapping the active faults. Faults which have a significant extensional component are described as 'normal', though it is recognized that these have an unknown component of strike-slip motion.

The line begins on the northern shelf of the eastern Çınarcık Basin. This unit is highly reflective, and little penetration occurs, so the internal structure is difficult to ascertain. Indications of a steep fault bounding the edge of the basin are apparent at CDP 1400. This may connect with the relatively continuous Northern Boundary Fault, which extends across the northern edge of the Sea of Marmara, linking the Çınarcık fault strand with the Saros-Gaziköy fault system. South of the fault, down to the base of the slope, is a series of convoluted sedimentary deposits (unit 2), possibly quite recent, though slightly deformed.

A S-dipping normal fault, which forms part of the edge of the basin, can be observed at CDP 1750. This fault continues under the seafloor and appears to connect at depth with a much steeper fault at CDP 1975. There is a considerable change in reflectivity across this steeper fault, yet the sedimentary horizons to the south do not seem to show any evidence of the tilting associated with normal fault block motion. It is therefore interpreted as having a strong strike-slip component. The sedimentary layers around the fault at CDP 1975 are coherent, indicating a relatively narrow zone of deformation. The unit between these two faults is slightly downthrown to the south, an indication of a more active fault further south. This unit can be observed more clearly further west, but is almost absent to the east, implying that the two faults are strands originating from a single fault to the east. The northernmost of these two strands is seen clearly on the succession of profiles to the west, and forms the Northern Boundary Fault.

To the south of CDP 2100 are relatively continuous flat-lying sediments, which form the bottom of the deep Çınarcık basin (unit 1). There is evidence for small flower structures, which are generally associated with strike-slip motion, as well as some small internal faulting within the unit, but these appear to have initiated relatively recently, with offsets of the order of tens of metres, and do not affect the long-term deformation in the area.

There is a N-dipping fault at CDP 3600, north of which the sedimentary horizons are quite flat, but south of which they drape over a unit of the attenuative chaotic reflector. This forms the southern edge of the basin. There is no evidence of tilting of the block to the south, because there are no strong reflections within it. The sediments above this unit are only slightly disturbed, indicating that little motion has taken place on the fault since they were deposited. The unit continues further south, until it terminates against a steep S-dipping fault, at CDP 4400. The deformation around this fault is localized, indicating that the motion has taken place on a single fault surface.

South of the fault at CDP 4400, the deeper basement unit is visible dipping south towards another major normal fault at CDP 7600. This half-graben is filled with sediment which shows small antithetic faults. The major fault at CDP 7600 appears to be *en echelon* with the Çınarcık strand of the North Anatolian Fault, which ruptured in August 1999, and is also responsible for the uplift required to lift Imralı Island above the surrounding Neogene sediment. The surface of the Island is flat and dips south, probably because it also has been rotated by movement on normal faults (Smith *et al.* (1995). The large offsets and activity, both recent and historical on the Çınarcık fault imply that it is more significant in transferring the right lateral strike-slip motion of the North Anatolian Fault Zone across the Sea of Marmara than the fault on the northern side of the Çınarcık basin.

The seafloor to the south of CDP 7600 is again quite reflective, and little penetration is achieved. Dipping basement features are seen, with more possible erosional surfaces underlying the infilling sediment. This sediment exhibits a flower structure faulting pattern around CDP 9600. These layers terminate abruptly against a fault plane at CDP 9950. This fault is thought to be the westward continuation of a strand of the Gemlik fault, although it is difficult to be certain because of the distance between the profiles. It may be an *en echelon* fault which becomes more active to the west as the Gemlik fault dies out.

By analysing the other lines in the dataset in a similar manner, and identifying the major units and faults across the basin, we generated a map of the active faults and the manner in which they contribute to the bathymetry in the Sea of Marmara (Fig. 1).

The depth of penetration into the subsurface and the resolution of the images has lead to a clearer understanding of the tectonics in the area. The survey conducted by Smith *et al.*

(1995) imaged the surface sedimentary layers clearly but their sparker data only penetrated to a depth of ~500 m. While the same features are present in both data sets, we are now able to see the full extent of some faults which were not clearly visible before, and also which faults have large vertical displacements.

Discussion

GPS measurements (Reilinger *et al.*, 1997) show that 60% of the present-day motion in the North Anatolian Fault zone is taken up on the Çınarcık fault strand in the east coast of the Sea of Marmara. This observation correlates well with the seismicity in the area (Ambraseys, 1988), and also with the seismic reflection data presented here (Fig. 2), which show that the southern shelf of the Çınarcık basin has no large active faults, whereas the northern basin shows rapid, large-scale subsidence with some accompanying sedimentary infilling. Unfortunately, the sediment infill has not yet been dated, so an estimate of the onset or rate on subsidence is not possible. A map showing the depth to the basement (Unit 3) would be useful, but is beyond the scope of this paper.

Continental extension is commonly distributed over a region that is broad in the direction of extension, whereas sheared motion is restricted to relatively narrow zones (England and Jackson, 1989). These features are reproducible in thin sheet viscous models of continental deformation, where models with extensional boundaries have aspect ratios of ~1–2, and aspect ratios for strike-slip boundaries are ~5–10. (England *et al.*, 1985). In accordance with these models, the GPS data show that the motion is relatively confined parallel to the strike of the North Anatolian Fault east of 31°E, whereas to the west, the E–W strike-slip faulting associated with the North Anatolian Fault becomes distributed over several faults that cross the Aegean with NE–ENE strike (Straub and Kahle, 1997). Both surface mapping and earthquake focal mechanisms indicate that the North Anatolian Fault Zone becomes more complex, with both strike-slip and extensional mechanisms west of 31°E (Reilinger *et al.*, 1997). GPS data, however, show that the motion vector changes from E–W to WSW somewhere west of Marmara Island, around 27.5°E. Between these two longitudes the trends of the faults are no longer parallel to the overall direction of motion. Why the motion should change direction here is not yet understood.

Conclusions

This survey has produced a more complete coverage of the Sea of Marmara than any dataset available for previous interpretation. Analysis of the profiles shows that:

1 Despite the increased coverage in the survey area the way in which the faults link across the Sea of Marmara is still unclear.
2 The S-dipping fault south of the Princes Islands appears to be much less important than the Çınarcık fault.
3 The deep basins are above the hanging walls of faults with large dip displacements. Most of the active normal faults dip N, with the sediments in their rotated foot walls dipping S.
4 The presence of the Sea of Marmara at the western end of the North Anatolian Fault is a direct result of localized N–S extension. This extension is thought to be due to the interaction between the strike-slip motion on the North Anatolian Fault, and the onset of influence of the Hellenic Arc.
5 The deformation across the northern Sea of Marmara is taken up by a series of *en echelon* faults from the Çınarcık fault, as it enters the sea from the east. This fault appears to have the largest normal component offset, as well as being the most seismically active, historically.
6 Within the sedimentary infill, antithetic faults and flower structures are observed. Also noted are faults which terminate against overlying layers, indicating reduced activity in some areas, where the motion is taken up on neighbouring faults.
7 The southern edge of the deep basins is defined by a series of *en echelon* faults which step across from the northern coast of Imralı Island to the northern coast of Marmara Island.

Acknowledgements

We thank the captain, officers, crew, and scientific party of the R/V *MTA Sismik 1*, for their assistance during the Marmara cruise in September 1997, and the Royal Society for funding this research. We also thank P. Huchon and J. Jackson for their comments and insights as reviewers. Earth Sciences contribution number 5522 [UC].

References

Ambraseys, N.N., 1988. Engineering Seismology. *Earthq. Engng Struct. Dynam.*, **17**, 1–105.
Barka, A.A. and Kadinsky-Cade, K., 1988. Strike-slip fault geometry in Turkey and it's influence on earthquake activity. *Tectonics*, **7**, 663–684.
Demets, C., Gordon, R.G., Argus, D.F. and Stein, S., 1990. Current plate motions. *Geophys. J. Int.*, **101**, 425–478.
England, P.C., Houseman, G.A. and Sonder, L.J., 1985. Length scales for continental deformation in convergent, divergent and strike-slip environments: analytical and approximate solutions for a thin viscous sheet model. *J. Geophys. Res.*, **90**, 3351–3357.
England, P. and Jackson, J., 1989. Active deformation of continents. *Ann. Rev. Earth Planet. Sci.*, **17**, 197–226.
Reilinger, R.E., McCluskey, S.C., Oral, M.B., King, R.W. and Toksoz, M.N., 1997. GPS Measurements of present day crustal movements in Arabia-Africa-Eurasia plate collision zone. *J. Geophys. Res.*, **102**, 9983–9999.
Şaroglu, F., Emer, O. and Kuşçu, I., 1992. *Active Fault Map of Turkey*. General Directorate of Mineral Research and Exploration, Ankara.
Şengör, A.M.C., 1979. The North Anatolian transform fault: its age, offset and tectonic significance. *J. Geol. Soc. London*, **136**, 269–282.
Şengör, A.M.C., Görür, N. and Şaroglu, F., 1985. Strike-slip faulting and related basin formation in zones of tectonic escape: Turkey as a case study. In: *Strike-slip Deformation, Basin Formation, and Sedimentation* (K.T. Biddle and N. Christie-Blick, eds). *Spec. Publ. Soc. econ. Paleont. Miner., Tulsa*, **37**, 227–264.
Smith, A.D., Taymaz, T., Oktay, F. *et al.*, 1995. High resolution seismic profiling in the Sea of Marmara (northwest Turkey): Late Quaternary sedimentation and sea-level changes. *Bull. geol. Soc. Am.*, **107**, 923–936.
Stolt, R.H., 1978. Migration by Fourier transform. *Geophysics*, **43**, 23–48.
Straub, C. and Kahle, H.G., 1997. GPS and geologic estimates of the tectonic activity in the Marmara Sea region, NW Anatolia. *J. Geophys. Res.*, **102**, 27,587–27,601.
Taymaz, T., Jackson, J. and McKenzie, D., 1991. Active tectonics of the north and central Aegean Sea. *Geophys. J. Int.*, **106**, 433–490.
Wong, H.K., Ludmann, T., Ulug, A. and Görür, N., 1995. The Sea of Marmara: a plate boundary sea in an escape tectonic regime. *Tectonophysics*, **244**, 231–250.

Received 25 March 1999; revised version accepted 8 November 1999

